



Research article

UDC 69

DOI: 10.34910/MCE.137.2



## Structural behavior of thin-walled steel short columns filled with recycled aggregate concrete

A.S. Haitham , H.N.A. Ali

The University of Kerbala, Karbala, Iraq

 [haitham.a@s.uokerbala.edu.iq](mailto:haitham.a@s.uokerbala.edu.iq)

**Keywords:** short length column, recycled aggregate concrete filled steel tubes, RACFST, recycled coarse aggregate, RCA, thin-walled steel tubes, axial compression, section shape effect

**Abstract.** This paper presents an experimental investigation to study the behavior of 12 recycled aggregate concrete-filled steel tubular (RACFST) short columns subjected to concentric axial loading. These columns formed from six different cross-sections involving: triangle, elliptical, and hexagon, whereas the other three sections included traditional forms for control purposes, involving: square, rectangular, and circular. The whole of the RACFST columns sections used is made of mild steel plates. All columns were divided into two groups and filled with recycled aggregate concrete. The steel tube thickness was the only parameter modified to study its effect properly. In addition, the study included the search for the best effective section with regard to the properties of stability and confinement, so these columns were designed so that the cross-sectional areas of steel tubes were approximately equal. Different data have been recorded in the experimental tests, including: the ultimate failure axial load, final failure stress, the reduction in the axial column length, failure patterns, and lateral displacement. Data obtained exhibited of RACFST columns with circular and elliptical sections, respectively, showed better stability, confinement for the concrete, and the ability to withstand greater final failure stress. On the other hand, the arrangement of all RACFST columns with polygonal sections in terms of bearing the ultimate failure stress was as follows: hexagonal (C.H.), square (C.S.), rectangle (C.R.), and triangle (C.T.). The reason for this was the increase in the number of corners of steel plates that formed the model. In another concept, this means that the greater the number of formed sides and the greater the angle between the sides ( $90^\circ$  or more), the section can achieve more stability and confinement, respectively. In addition to these, the results showed, when the thickness of the steel tube increases, the concrete contribution ratio value decreases of the specimens examined.

**Citation:** Haitham, A.S., Ali, H.N.A. Structural behavior of thin-walled steel short columns filled with recycled aggregate concrete. Magazine of Civil Engineering. 2025. 18(5). Article no. 13702. DOI: 10.34910/MCE.137.2

### 1. Introduction

Recycled aggregate concrete-filled steel tubes (RACFST) are a type of composite construction consisting of two main sections: recycled concrete using recycled aggregate concrete (RAC) as a filler and hollow steel tube. These hollow steel tubes are manufactured in several ways, either by cold forming, steel plate welding, or hot rolling, as reported in *Concrete-filled Tubular Members and Connections* by X.-L. Zhao, L.-H. Han, H. Lu [1]. Common sections used in these columns are circular, square, and rectangular and are often called "circle hollow section (CHS)", "square hollow section (SHS)", and "rectangle hollow section (RHS)". Concrete-filled steel tubes (CFST) have many features and benefits for different buildings, including high resistance to force and fire, preferred ductility, and the unique ability to absorb energy, in addition to the lack of the need to use shutters during concrete construction, and as a result, reducing the cost and time of construction work. These advantages have been utilized in a wide field and led to the expanded use of this technique in civil engineering structures [2]. Through a previous statistical study concerning the 100

tallest buildings in the world according to materials, it was found, without a doubt, that the need to use these composite structures will increase shortly, while steel towers continue to decline, which calls for research in this regard [3].

The tensile strength of concrete is less than compressive strength. In addition, under two- or three-axial restraint pressure, the compressive strength is better. The tensile strength is high for steel structures, but the shape is likely to have local buckling under compression.

In CFST, the properties of each material have been harnessed, and working together leads to its wonderful benefits. The confining pressure of the concrete is provided by the steel tube, in turn, the concrete core reduces the local buckling of the steel tube.

The ideal and commonly used forms of sections in steel columns filled with concrete are square, rectangular, and circular, as each type of these sections has its characteristics. The cross-section of the circular column gives strong confinement of the filled concrete, also the probability the local buckling occurred in SHS or RHS cross-sections even though CFST with SHS and RHS sections are still in great use in various construction sectors because it is easier to design and connect between columns and has high rigidity against sectional bending [2].

Other cross-sections with special shapes such as hexagonal, elliptical, and triangular are used for many reasons related to aesthetics, availability of raw materials, ease of manufacture, and low cost [4]. Therefore, the columns of the shapes of these sections were the focus of the researcher's study by comparing their behavior with the columns of commonly used sections such as circular, square, and rectangular.

Previous studies showed that CFST column with elliptical section has higher strength and rigidity than hollow steel tube columns with the same cross-sectional shape. Concrete filler reduces the local buckling that may occur in steel tubes, which promotes the use of thin-walled CFST columns [5]. The short CFST column has shown that the shape of the hexagonal steel tube column approximates that of the circular column, as both work to confine the concrete more closely along the circumference thus enhancing the strength and ductility of the composite tube [6]. The effect of confinement was important in CFST stub columns with circular sections filled with normal strength concrete (NSC), but in rectangular columns, the effect of confinement was not very significant, as the theoretical capacity of the cross-section was overestimated compared to its real capacity [7]. The intermediate CFST columns with octagonal cross-sections showed the greatest final failure stress after when have been evaluated with all examined specimens [8]. The hierarchical arrangement in terms of sectional shapes of CFST columns associated with maximum bearing capacity and energy absorption capacity is circular, rectangular, and square. It also showed that the increase in the thickness of the steel tube leads to an increase in the maximum bearing capacity, energy absorption capacity, and stiffness [9].

Many previous experimental studies have proven the possibility and sufficiency of using RAC in structural buildings in various sectors of civil engineering, despite the initial shortcomings of recycled concrete related to the lack of some of its mechanical properties such as low compressive strength, modulus of elasticity, toughness, energy dissipation in return for strain greater peak, higher Poisson's ratio, creep, and shrinkage compared to natural aggregate concrete (NAC) [10–16]. Therefore, a lot of efforts have been made by previous researchers to enhance the using the mechanical behavior of RAC in construction structures.

Chen et al. [17] reported that the researchers Konno et al. were the first in this field when introduced the idea of using recycled concrete as a filler in steel tubes. The target of this was to improve the mechanical properties of RAC.

One of the most remarkable properties of recycled coarse aggregate (RCA) is its high ability to absorb water when it is not previously wet compared to natural coarse aggregate. RCA works to reduce the percentage of water in mixed concrete and thus increases the strength of the concrete [18].

This feature was confirmed by Chen et al. in [17], reached in their study that by increasing the content of the non-pre-wet coarse aggregate, the compressive strength of the RACFST columns is enhanced. Then by increasing the percentage of the wet coarse aggregate, the compressive strength of these columns decreases. At the same time, they have shown in their study that the use of RAC in CFST as a structural material is possible and safe.

Safiuddin et al. [19] have shown that recycled coarse aggregate concrete (RCAC) can be used completely instead of natural coarse aggregate to obtain concrete with strength ranging 80–90 % of the strength of natural coarse aggregate concrete. Azevedo et al. [20] explained that the resistance of a composite column depends not only on the compressive strength of concrete but as well on the ratio between the compressive strength of both steel and concrete, i.e.  $(f_y/f_c)$ , besides to that, they stated the

confinement effect confirmed to be a significant factor in the strength of the RACFST column. Yang & Han [21] presented experimental studies on the behavior of RACFST columns filled with RAC, they mentioned the failure of all specimens is failure buckling. Also, they illustrated that the failure patterns for those columns were similar to counterparts in CFST columns, and, the behavior of all tested specimens was ductile behaved. Yang & Han [22] showed that the behavior of failure patterns and compressive strength of RACFST columns were similar to that of hollow steel tubes filled with normal concrete. Also, they mentioned needing further investigation in this zone.

Chen et al. [23] showed that the failure modes of square RACFST columns were similar to CFST having the same cross-section filled with normal concrete (NC). Li et al. [24] mentioned the possibility of using RAC with CFST columns structural applications. Also, they mentioned that the researchers B. Qiu et al. presented experimental investigations regarding the behaviour of RACFST columns under the axial compression with square and circular cross-sectional shapes and made of thin walls. They explained that the patterns of failure and deformation of these columns are similar to those found in CFST columns filled with natural aggregate. In addition to that, there is also an accepted consensus that the structural behaviour of RACFST columns is slightly less than that of CFST columns filled with NAC.

Wang et al. [25] showed that the experimental results listed a reduction in compressive strength of RACFST of a lower 10 %, this happened due to the use of RCA. Niu & Cao [26] – that the results showed the damage occurring and failure modes of RACFST columns with circular and squared cross-sections were similar to those of CFST columns filled with NC. Besides that, the results showed that the columns with circular cross-sections have the greater load-bearing capacity and better resistance to deformation compared to square-section columns that have the same cross-sectional area of concrete, material strength, and steel ratio. Also, using RAC instead of NC has a lesser effect on the axial compression of square columns compared to circular columns.

Lyu et al. [27] showed that the compressive strength and modulus of elasticity of the circular and square RACFST columns decrease when using RCA instead of NC. Yang et al. [28], through their study of 16 rectangular cross-sections RACFST columns subjected to axial stress, concluded that the deformation behavior and failure mode of these columns were similar to their counterparts of CFST columns filled with NC. Moreover, the authors stated that the RACFST column is a composite column that combines the mechanical efficiencies of CFST columns with the environmental and economic advantages of RAC.

Here, it is important to be noted that the importance of this research lies in benefiting from each of the mechanical properties of recycled concrete and thin-walled hollow steel tubes. Improving these properties with the common work of both materials through composite columns and thus the effectiveness of these structural members increases.

In addition, this study investigated some forms of special cross sections for thin-walled steel columns and tried to find the optimal section in terms of stability and confinement, while comparing it with the commonly used sections. Moreover, achieving the requirements of architecture from an aesthetic point of view, by providing sections with special shapes, while providing the required information about the possibility of using them in various sectors of civil engineering.

Finally, in this research, RCA was used as fillers for these columns, due to its great importance in promoting environmental conservation. Through reducing the depletion of natural resources, preserving the environmental diversity of living organisms, reducing environmental pollution of the land and air, and reducing noise. Also, recycled aggregate (RA) is undoubtedly of great importance in several aspects, including reducing costs compared to continuing to use natural aggregate, and helping to get rid of the rubble of old or destroyed buildings due to wars and natural disasters. The possibility of using recycled concrete, including coarse aggregate, in the building and construction can effectively contribute to the promotion and development of sustainability. As it is known, achieving sustainability is a prerequisite for modern construction, and thus achieving comprehensive quality of use to achieve the well-being of humanity without compromising the natural resources that can be provided for future generations.

By reviewing previous studies, it was noted that there was no extensive coverage to show the effect of changing the thickness of the steel tube on the ultimate stresses in the serviceability limits of RACFST columns. Especially when comparing these stresses for the same cross-section shape for all sections (circular, elliptical, hexagon, square, rectangular, and triangle), which have been used in the field of construction. In addition, the effect of the cross-section shape in terms of the number of ribs that formed the model's shape and the angles between these ribs on the ultimate bearing capacity of these columns has not been extensively studied. Therefore, here in this research, the effect of the variables mentioned above was studied. The following main goals in this manuscript are adopted.

1. Researching the best effective cross-sectional shape for all RACFST columns when using RCAC concerning the properties of stability, confinement, and ultimate stress in the serviceability limits,

- for special shapes such as hexagonal, elliptical, and triangular and compare them, with columns with conventional cross-sectional shapes such as circular, square, and rectangular.
- Investigating about the hierarchical arrangement in terms of the maximum capacity to withstand the ultimate stress in the serviceability limits for the RACFST columns with polygonal cross-sectional shapes such as hexagonal, squared, rectangular, and triangular.
  - Provide practical experiments on the structural behavior of thin-walled steel short columns filled with RCAC under axial compression because so far, the numerical and experimental studies related to the compressive behavior of RACFST columns are insufficient. In addition, no design methods for local stability are available, for those columns.

## 2. Materials and Method

After a detailed study of the previous literature, the materials required for both mild steel plates and concrete made of RAC needed in the experimental work were identified and provided. Then, a total of 12 samples were proposed. The shapes of the cross-sections of hollow steel tubes proposed for these samples and their details are shown in Fig. 1 and Table 1, respectively.

### 2.1. Description of Hollow Steel Tubes Specimens

The columns specimens that were used in this study are twelve RACFST columns with six different cross-sections, three of which are commonly used for comparison purposes, which are circular, square, and triangle. But the other remaining, are special sections, and they included the elliptical, the hexagon, and the triangle as shown in Fig. 1.

To identify all RACFST specimens, these symbols ("C.C.", "C.H.", "C.E.", "C.S.", "C.R.", and "C.T.") were used, where the first letter represents the composite column specimen and the second letter denotes to circular, hexagonal, elliptical, square, rectangular, and triangle, respectively.

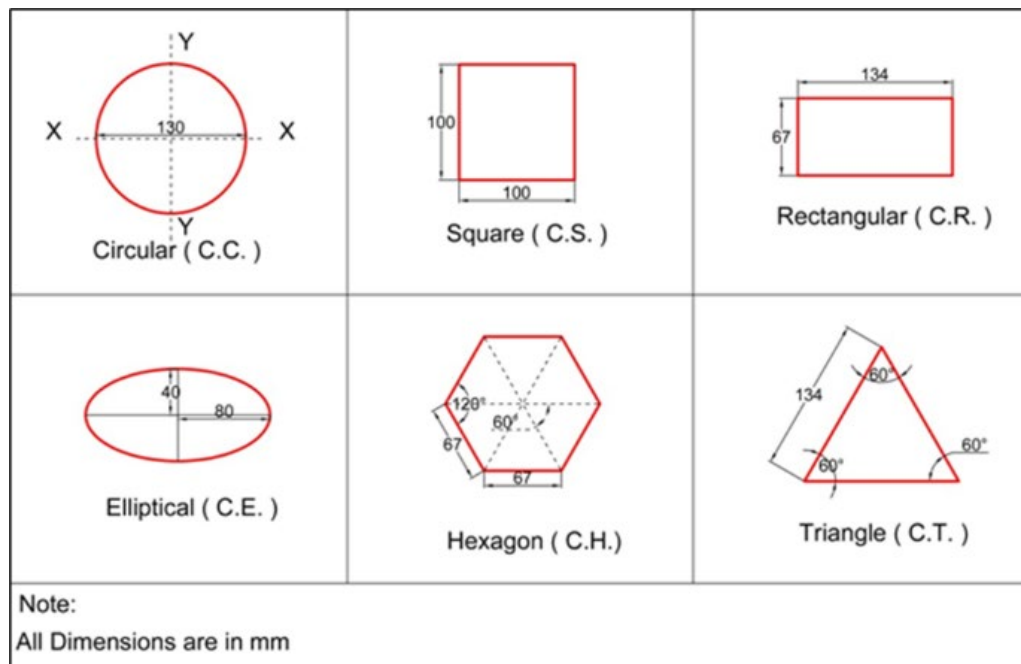


**Figure 1. Various cross sections of RACFST columns.**

All specimens were divided into two groups: the first group with a thickness of  $t = 1$  mm, whereas the second group with a thickness of  $t = 2$  mm. Sections of all RACFST columns were designed with approximately an equal external perimeter ( $P$ ) so, thus this parameter does not affect the conclusions obtained from the cross-section shape effect analysis. The length ( $L$ ) of each specimen was 300 mm, while the  $P$  of the cross-section of each column was 400 mm, with a difference of 2–3 %. The information for these specimens was recorded in Table 1.

**Table 1. Data obtained from the proposed design of the RACFST columns models.**

Group no.	Section's shape	Symbols	$P$ mm	$L$ mm	$t$ mm	$A_s$ mm <sup>2</sup>	$A_c$ mm <sup>2</sup>
G1	Circle	C.C.	408	300	1	408	13273
	Hexagonal	C.H.	402	300	1	402	11663
	Ellipse	C.E.	388	300	1	388	10053
	Square	C.S.	400	300	1	400	10000
	Rectangle	C.R.	402	300	1	402	8978
	Triangle	C.T.	402	300	1	402	7772
Group no.	Section's shape	Symbols	$P$ mm	$L$ mm	$t$ mm	$A_s$ mm <sup>2</sup>	$A_c$ mm <sup>2</sup>
G2	Circle	C.C.	408	300	2	816	13273
	Ellipse	C.E.	388	300	2	776	10053
	Hexagonal	C.H.	402	300	2	804	11663
	Square	C.S.	400	300	2	800	10000
	Rectangle	C.R.	402	300	2	804	8978
	Triangle	C.T.	402	300	2	804	7772

## 2.2. Experimental Method and Properties of the Materials

### 2.2.1. Ordinary Portland Cement

Ordinary Portland Cement (OPC) in this experimental work was used as shown in Fig. 2.



**Figure 2. Ordinary Portland Cement used in this study.**

This type of cement was kept in a dry place to avoid exposure to moisture. The test results showed that the cement conformed to Iraqi Standard No. 5/1984 [29]. Tables 2 and 3 show the physical properties and chemical composition of cement, respectively.

**Table 2. Physical properties of OPC.**

Physical properties	Test result	Iraqi specification No. 5/1984
Fitness (m <sup>2</sup> /kg)	398	Not less than 230
Initial setting (min.)	174	Not less than 45 min.
Final setting (hr.)	04:55	Not more than 10 hr.
Compressive strength (MN/m <sup>2</sup> ) for cement paste at 3 days of age	25.6	Not less than 15

at 7 days of age

35.2

Not less than 23

**Table 3. Chemical composition of OPC.**

Compound composition	Chemical composition	Weight (%)	Iraqi specification No. 5/1984 %
Lime	Ca O	62.6	–
Silica	SiO <sub>2</sub>	19.3	–
Aluminum oxide	AL <sub>2</sub> O <sub>3</sub>	4.5	–
Iron oxide	Fe <sub>2</sub> O <sub>3</sub>	4.7	–
Magnesia	MgO	4.1	5 % max
Sulfate	SO <sub>3</sub>	1.8	2.5 % max
Loss on ignition	L.O.I	1.6	4 % max
Insoluble residue	I.R	0.6	1.5 % max
Lime saturation factor	L.S.F	0.9	0.66–1.02
Tricalcium Aluminates	C <sub>3</sub> A	4	–
Tricalcium Silicate	C <sub>3</sub> S	65.2	–
Dicalcium Silicate	C <sub>2</sub> S	6.1	–
Tetra calcium alumina ferrite	C <sub>4</sub> AF	14.5	–
Chloride	CL	0.04	0.1 max
Aluminum oxide Iron oxide	AL <sub>2</sub> O <sub>3</sub> / Fe <sub>2</sub> O <sub>3</sub>	0.9	–

### 2.2.2. Fine Aggregate (Sand)

Fine aggregate with an optimum grain size of 4.75 mm has been used for the concrete mixtures in this investigation as shown in Fig. 3.



**Figure 3. Fine aggregate (sand) used in this study.**

The chemical and physical properties of this sand comply with what is required according to the Iraqi standard specification (IQS) No. 5/1984 [29]. The harmful, soft materials, the gradient, and chemical properties of this type of sand are shown in Tables 4 and 5, respectively.

**Table 4. Harmful and soft materials in fine aggregate (sand).**

Property	Test result	Specification limits % Iraqi specification No. 45/1984
Material passing through 75 pm sieve	3.3 %	< 5 % max.
Sulfate content (SO <sub>3</sub> )	0.089 %	< 0.5 % max.

**Table 5. The grading of fine aggregate (sand).**

Sieve size (mm)	Passing accumulative %	Specification limits % Iraqi specification No. 45/1984
10	100	100
4.75	97	100–90
2.36	85	100–85
1.18	71	100–75
0.6	61	79–60
0.3	32	40–12
0.15	7	10–0

### 2.2.3. Recycled Coarse Aggregate (Gravel)

The waste concrete, which resulted from the demolished concrete buildings, was the resource of the RCA. Concrete pieces with lengths ranging 400–500 mm was brought to the University of Karbala laboratory. After that, these pieces were smashed into small pieces by a laborer using a hand hammer. The aggregate used was determined to be with grading range 5–19 mm because the hollow steel tube samples were made with a small-scale size. This aggregate was separated by analyzing the sieve according to the above gradation. After that, the required quantities were weighed by using a sensitive electronic balance. These aggregates were soaked in water for 24 hours to get the saturated surface condition before mixing [28]. Fig. 4 illustrates the above steps in the preparation of RA. RCAC with NSC of 25 MPa was the material proposed as a filling material in all hollow steel tubes.



**Figure 4. Preparation stages of recycled coarse aggregate and devices used.**

Tables 6 and 7 shows the gradient test results and the chemical properties of RCA (gravel) that comply with Iraqi Standard No. 45/1984 [30]. The test result found that the SO<sub>3</sub> sulfite content (0.06 %) is acceptable within the limits of the Iraqi Standard mentioned above, which is allowing a maximum of 0.1 %.

**Table 6. Grading of coarse aggregate.**

Sieve size	Grading of sample passing %	Specification limits % Iraqi specification No. 45/1984
19.5	100	95–100
9.5	45	30–60
4.75	4	0–10

**Table 7. Chemical properties of coarse aggregate.**

Property	Test result	Specification limits % Iraqi specification No. 45/1984
Material Passing 75 pm Sieve	0.3 %	< 3 %
Sulfate content (SO <sub>3</sub> )	0.06 %	< 0.1 %

#### 2.2.4. Water of Mixing

Tap water was used in all preparations of a fresh green concrete mixture, as well as the curing process of all specimens.

#### 2.2.5. Trial Mixing to the Materials of Concrete

After complete, from all these tests, three mixing trials of the materials of concrete have been carried out to find the best proportion to achieve the target compressive strength, which is 25 MPa. Firstly, three cubes of concrete with dimensions of 15 × 15 × 15 cm were cast for each mixture to evaluate the degree of compressive strength of the concrete according to BS 1881: Part 116-1989 as reported in [29]. After 24 hours of casting these cubes, they were removed from their iron molds and placed in special water basins to complete the curing process for these samples. The average compressive strength of these cubes at the age of 28 days was taken through testing in the laboratory using a digital testing machine. Fig. 5 illustrates the above steps. In Table 8, the average value of the ultimate compressive strength of cylinder ( $f^c$ ) and the average value of the ultimate compressive strength of cube ( $f^{cu}$ ) obtained from tests have been listed.

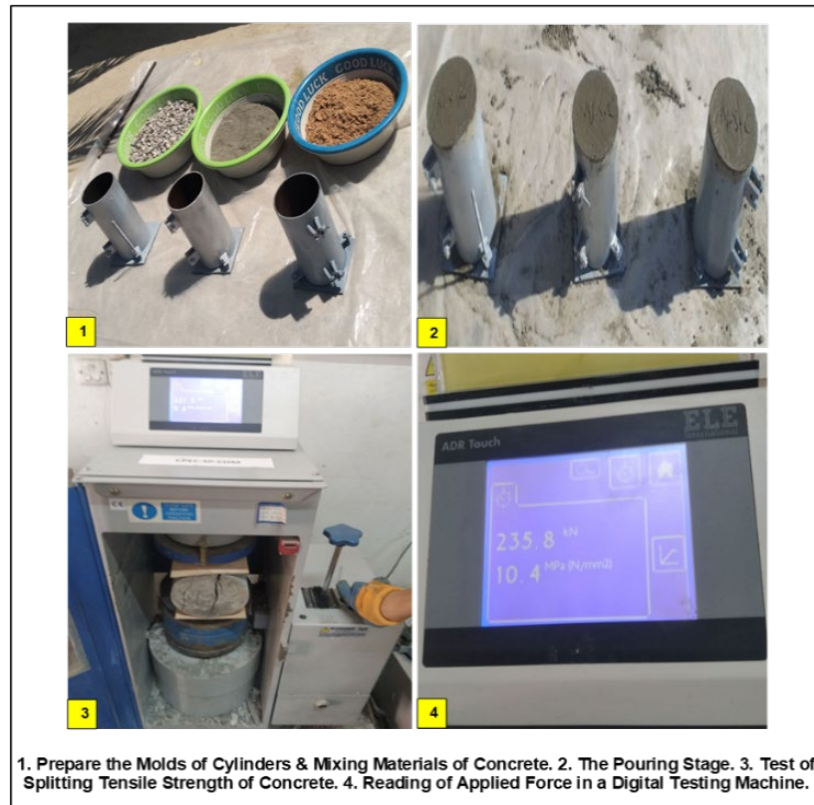


Figure 5. Steps of three mixing trials of concrete to achieve the target compressive strength.

Table 8. Weights of mixing NC materials per cubic meter  $\text{kg/m}^3$ .

Trial no.	Cement kg	Sand kg	R.C.A(Gravel) kg	W/C	Weight ratios for mixing	Average $f_{cu}$ MPa	Average $f_c$ MPa
1	350	650	850	0.40	1:1.857:2.43	27.075	21.65
2	300	600	900	0.42	1:2:3	31.25	25
3	375	600	1100	0.45	1:1.6:2.93	40	32

After obtaining the target compressive strength of 25 MPa, where was the mixture selected with the ratio (cement: sand: RA) for  $1 \text{ m}^3$  was ( $300 \text{ kg/m}^3$ ;  $600 \text{ kg/m}^3$ ;  $900 \text{ kg/m}^3$  is 1:2:3), respectively, with the water-cement ratio  $W/C = 0.42$ . Finally, three cylinders with a diameter of 15 cm and a height of 300 mm were cast, and the average splitting tensile strength after 28 days was taken according to ASTM C496 [29]. Fig. 6 illustrates the above steps. From this proportion, the average splitting tensile strength of this concrete mixture for three cylinders was 3.18 MPa.



**Figure 6. Steps of pouring three cylinder and test of splitting tensile strength of concrete.**

**2.2.6. Mechanical Properties of Steel Plate.**

To find the mechanical properties of the steel plate, which was used to manufacture the hollow steel tubes, standard coupon tensile tests have been carried out, which comply with the specification of American Steel Testing Materials (ASTM A370-22) (31). Fig. 7 shows the dimension of standard coupon as per ASTM-A370.

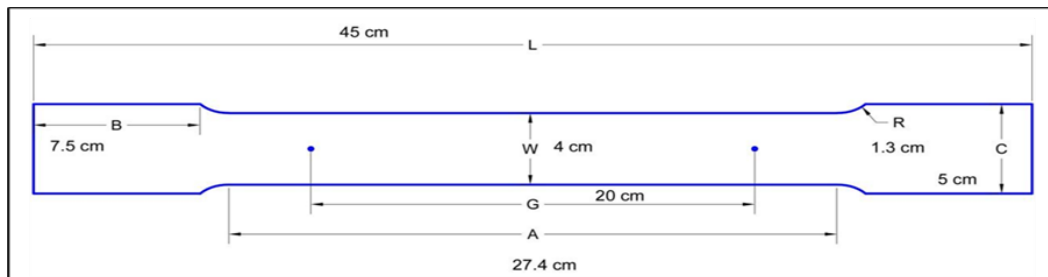


**Figure 7. Dimension of standard coupon as per ASTM-A370.**

The results of testing average ultimate failure stress, yield strength, and modulus of elasticity of three steel coupons with two thicknesses of 1 and 2 mm were 368 MPa, 258 MPa, 217 G Pa and 340 MPa, 258 MPa, 217 G Pa, respectively. The information for these Standard coupons test was recorded in Tables 9 and 10.

**Table 9. Properties of the steel coupon with a thickness of 1 mm.**

No. of coupon	Yielding stress ( $F_y$ ) Mpa	Ultimate stress ( $F_u$ ) M pa	Elongation at fracture %	Modulus of elasticity ( $E_s$ ) G pa	Thickness (t)
1	266	380	30.17	219	1
2	257	366	31.22	217	1
3	251	358	32.2	215	1
Mean	258	368	31.19	217	1

**Table 10. Properties of the steel coupon with a thickness of 2 mm.**

No. of coupon	Yielding stress ( $F_y$ ) Mpa	Ultimate stress ( $F_u$ ) M pa	Elongation at fracture %	Modulus of elasticity ( $E_s$ ) G pa	Thickness ( $t$ )
1	268	353	27	220.8	2
2	255	336	27.9	214.7	2
3	251	331	29	215.5	2
Mean	258	340	27.96	217	2

**Figure 8. Setup of steel coupons for a typical tensile test and types of equipment, and devices used.**

### 2.3. Manufacturing of Specimens

Specimens of RACFST columns represented the RACFST are a type of composite construction consisting of two main sections: recycled concrete using RA as a filler and hollow steel tubes. In current analysis, these hollow steel tubes were manufactured by steel plate welding.

#### 2.3.1. Manufacturing of Hollow Steel Tubes

Using the AutoCAD program, the cross sections of the columns were drawn according to the required measurements. After that, these cross sections and other parts of hollow steel tubes were cut from thin steel plates by using a CNC metal cutting machine as shown in Fig. 9.



**Figure 9. Shows the CNC metal cutting machine setup, control system, and devices used, with cross-sections of specimens and other parts.**

Based on these sections, the hollow steel tubes were formed according to the required shapes.

Each sample has been formed from two symmetrical parts so that its longitudinal welding is also symmetrical as shown in Fig. 10-8.

A steel plate with a thickness of 2 mm and dimensions 20 × 20 mm was welded as a base for these specimens as shown in Fig. 10-4. This base provides three-side confining conditions and prevents the leakage of fine materials from the specimens for the concrete mixture and increases its stability.



**Figure 10. Manufacturing steps of hollow steel tubes and types of equipment used.**

### 2.3.2. Pouring Stage of Hollow Steel Tubes

According to [32], green concrete (GC) is a type of concrete that includes at least one component made from waste, has an environmentally friendly production process, boasts high performance, and a sustainable life cycle. GC mix was used, with RCA for mixing instead of using NCA. The GC mixture was designed with a compressive strength of 25 MPa. The hollow steel tubes were prepared and cleaned from the inside before pouring to achieve a strong bond between the concrete and the steel tube as illustrated in Fig. 11a. The tubes were filled with prepared concrete in three layers. Each layer was compacted when filled with a metal compacter bar with several blows ranging 25–35 times so that the number of blows was distributed evenly on the surface of the concrete to get rid of air voids and obtain well-compressed concrete. After completing the top layer of each tube, the surface of the mold was flattened using a steel trowel as illustrated in Fig. 11b. The specimens in the molds were protected with nylon covers to prevent the evaporation of water from the fresh concrete after pouring. These specimens were left for 24 hours in a place with a temperature of 15–20 °C for a period of 24 hours to dry, and away from any vibrations as shown in Fig. 11c.

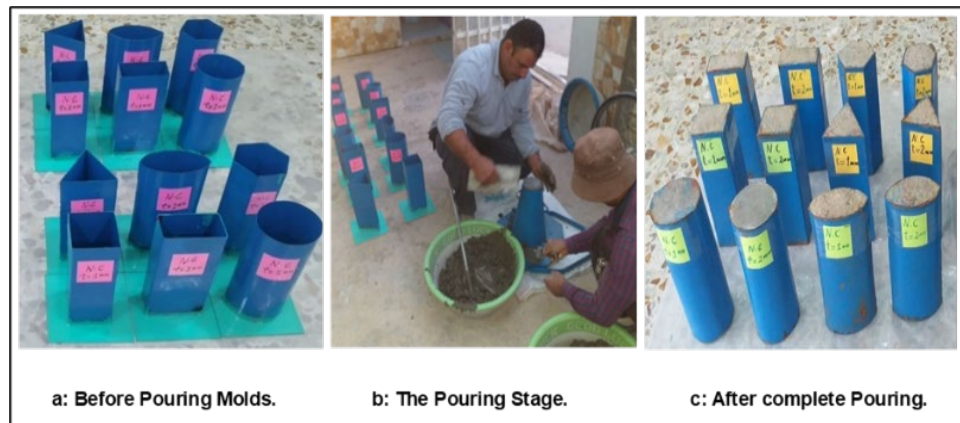


**Figure 11. Preparation of the pouring specimens process of RACFST columns.**

Finally, these samples were taken and immersed in a hot water basin at 60 °C for three days and then at 25 °C for a period of 28 days of age for completing the curing process as shown in Fig. 12a [33]. The base plates were removed from the samples after 48 hours after the completion of the pouring process for these samples as illustrated in Fig. 12b.

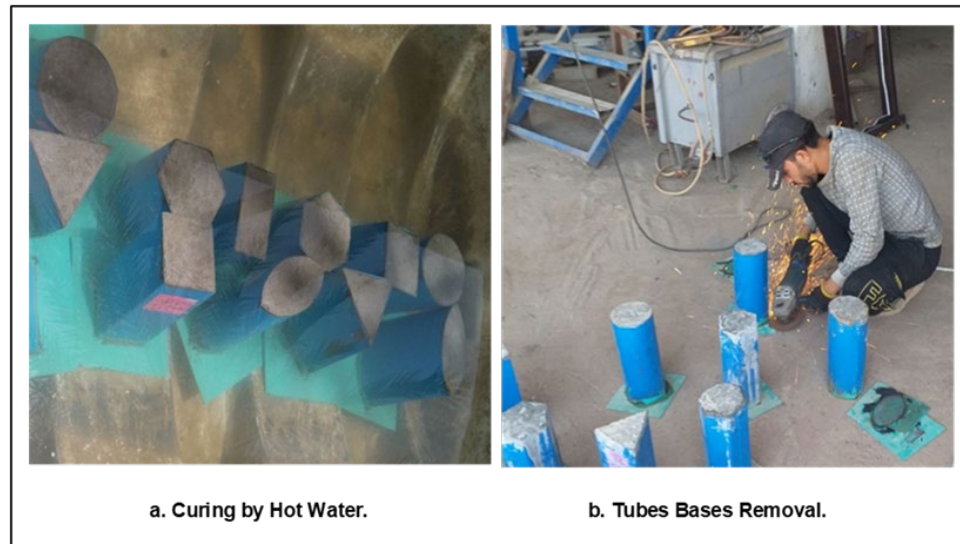


**Figure 12. Shows the process of curing concrete and removing bases plates from specimens.**

Moreover, the uneven surfaces of some samples were smoothed to ensure that the applied axial load was transmitted at the same time to both the steel tube and the concrete during the test as shown in Fig. 13.



**Figure 13. Shows smoothing surfaces of some samples.**

## 2.4. Test Setup

Before starting to apply axial compression on the samples, was checked that the test device and other connected devices with the control system are working properly. Next, was verified that the applied load could be applied to the specimens without occurring eccentricity. This was achieved by checking the flatness of the device surface. In addition to that, have been made sure that the center of the device's load cell matches the center of the sample to be examined.

The test included a study of the failure's patterns, the ultimate load for each sample, the vertical deformation, the transverse deformation, the effect of steel tube thickness on the maximum load, and the effect of cross-section shape on value of the ultimate load.

Three linear variable differential transformers (LVDT) devices have been used to measure the deflection in the sample due to the applied vertical load. One of them is to measure vertical deflection, the second is to measure the horizontal movement on the long side of the model and the third is to measure the horizontal movement on the other side of the model. All of them are installed in the middle of the column. The axial load was applied to all samples, in the same way. A hydraulic compressor presses the sample vertically from the top using the load cell. Fig. 14 shows the RACFST column with a rectangular cross-section under the test. The load was regularly increased by 10 kN until failure or when a sudden collapse occurred to the specimen. Finally, the axial load was applied by a load cell with a maximum capacity of 2000 kN linked to the computer. Fig. 15 shows one of the examined RACFST columns specimens in the testing machine with a schematic view with all details.



**Figure 14. Location of LVDT devices on RACFST column with a rectangular cross-section under the test.**

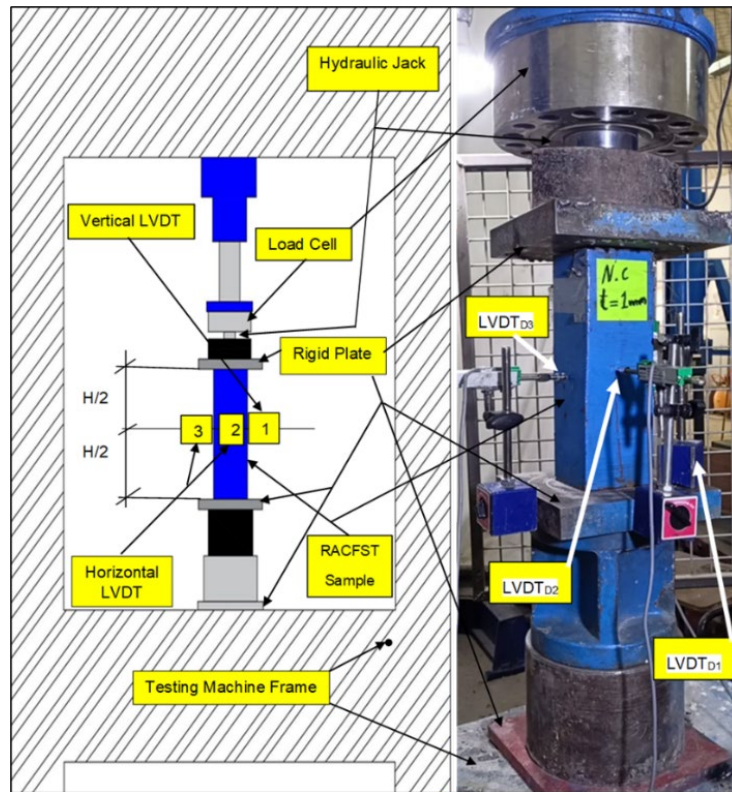


Figure 15. Detail of the testing machine and schematic view setup for one of the RACFST columns.

### 3. Result and Discussion

#### 3.1. Experimental Results

Data on ultimate failure axial load ( $N_u$ ) have been recorded in the experimental tests, while other information including: the ultimate stress ( $\delta u$ ), strength index ( $SI$ ), ductility index ( $DI$ ), and concrete contribution ratio (CCR), which are discussed later in detail, were obtained by some mathematical approaches. The information for these specimens was recorded in Table 11.

Table 11. Data obtained from the specimens test of RACFST columns.

Group no.	Sec. shape	Sym.	$P$ mm	$L$ Mm	$t$ mm	$A_s$ mm <sup>2</sup>	$A_c$ mm <sup>2</sup>	$N_u$ kN	$\delta u$ MPa	$SI$	$DI$	CCR
G1	Circ.	C.C.	408	300	1	408	13273	556.534	241.2	1	2.02	5.28
	Hexa.	C.H.	402	300	1	402	11663	430.763	206.9	0.857	1.63	4.15
	Elli.	C.E.	388	300	1	388	10053	391.095	211.8	0.878	1.46	3.90
	Squa.	C.S.	400	300	1	400	10000	329.261	177.6	0.736	1.58	3.19
	Rect.	C.R.	402	300	1	402	8978	269.144	156.6	0.649	1.37	2.59
	Tria.	C.T.	402	300	1	402	7772	189.758	122	0.505	1.44	1.82
Group no.	Sec. shape	Sym.	$P$ mm	$L$ Mm	$t$ mm	$A_s$ mm <sup>2</sup>	$A_c$ mm <sup>2</sup>	$N_u$ KN	$\delta u$ MPa	$SI$	$DI$	CCR
G2	Circ.	C.C.	408	300	2	816	13273	614.530	218.1	1	1.54	2.91
	Elli.	C.E.	388	300	2	776	10053	510.508	218.9	1.003	1.46	2.54
	Hexa.	C.H.	402	300	2	804	11663	460.924	178.3	0.817	1.26	2.22
	Squa.	C.S.	400	300	2	800	10000	390.701	165.9	0.760	1.78	1.89
	Rect.	C.R.	402	300	2	804	8978	330.900	148.9	0.683	1.51	1.59
	Tria.	C.T.	402	300	2	804	7772	278.710	135.4	0.621	3.78	1.34

### 3.2. Observation of Tested Specimens and Failure Patterns

For all the tested columns have been behaved, ductile failure was noticed. The tested short RACFST columns failed due to the internal cracking that occurred in the core of the concrete and then the crash of the recycled concrete – where the sounds of this crashed concrete were heard when exceeding the middle stages of loading – and then the lateral expansion. Continuing with the loading, a local outward buckling occurred near the middle of the RACFST columns as a result of the thin steel plates yielding. In the later stages of the applied loading, more external local buckling occurred near the top and bottom edges of the tested columns.

The failure patterns of all tested column specimens are shown in Fig. 16 for steel tube plates 1 and 2 mm, respectively. In general, the section shape had a distinctive effect on patterns of failure that have occurred in tested specimens, as the failure patterns of polygonal cross-sections such as hexagonal, squared, and rectangular were slightly different from the patterns of circular and elliptical sections. Furthermore, the RACFST sample with a triangle cross-sectional shape had not similar failure behavior to the remaining shapes. For illustrate, the mechanism of failure for these columns has been shown below.

Concerning the sample with a circular cross-section, swelling occurred in the lower half of the column due to the crushing of concrete, then the yielding of the steel resulting in local buckling near the upper end of the sample. Similarly, in the sample with an elliptical cross-section, the local buckling occurred in the middle of the column due to concrete crushing and expansion towards the steel tube. Moreover, local buckling occurred near the upper end of the sample during the last loading stages.

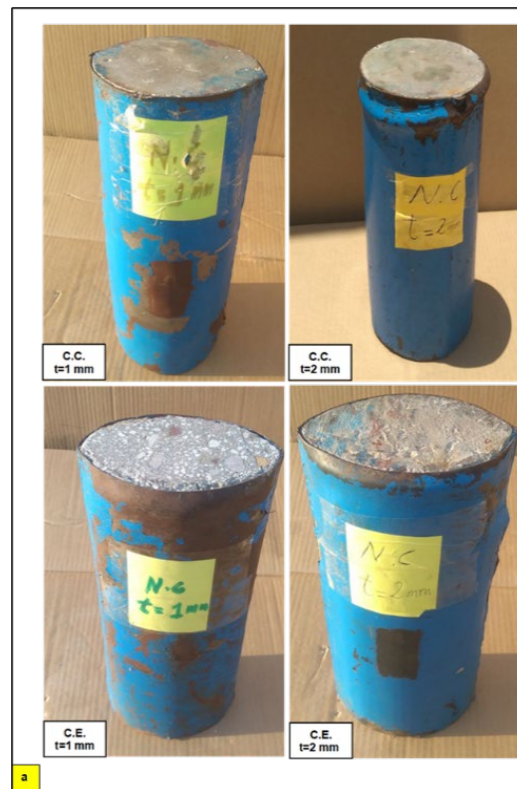


**Figure 16a. Failure patterns of tested RACFST columns of circular and elliptical cross section of steel tube thickness  $t = 1$  and  $2$  mm.**

While the sample with a hexagonal cross-section, limited local buckling occurred only at the end of the upper third of the specimen's length. This behavior indicates that the RACFST column with a hexagonal cross-section is less damaged than the other columns when subjected to concentric axial loading up to the failure stage of the column. In the sample with a square cross-section, multiple local buckling occurred, starting from the end of the upper third of the column to its end. With loading continued, welding failure occurred in the middle region of the column (corner of the column) due to the weak ductility of the weld. In the sample with a rectangular cross-section, local buckling occurred at the beginning of the lower third of the column.

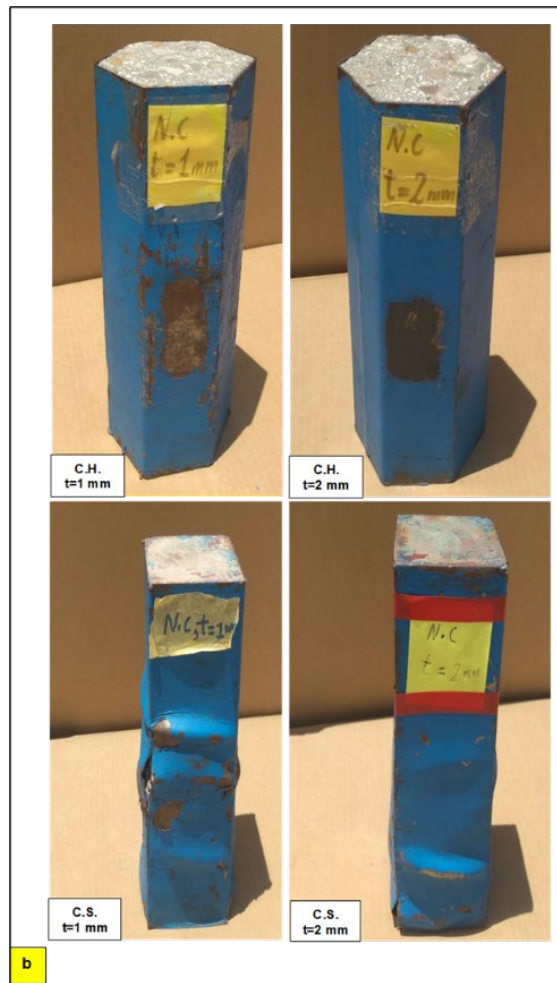


**Figure 16b. Failure patterns of tested RACFST columns of a hexagonal and square cross-section of steel tube thickness  $t = 1$  and  $2$  mm.**

The RACFST sample with a triangle cross-sectional shape had not similar failure behavior to the remaining shapes. Where simple local buckling occurred at the beginning of the lower third of the column. After that, with increasing load, local buckling occurred along the lower circumference of the base of the column.

But the values of the plastic deformation limit ( $DL$ ) of specimens were almost equal for the first and second groups. Except for the column with a circular cross-section, which gave higher results in a set of a thickness  $1$  mm. Besides, the column with a triangular cross-section gave a double value in a set with a thickness  $2$  mm as recorded in Table 11.

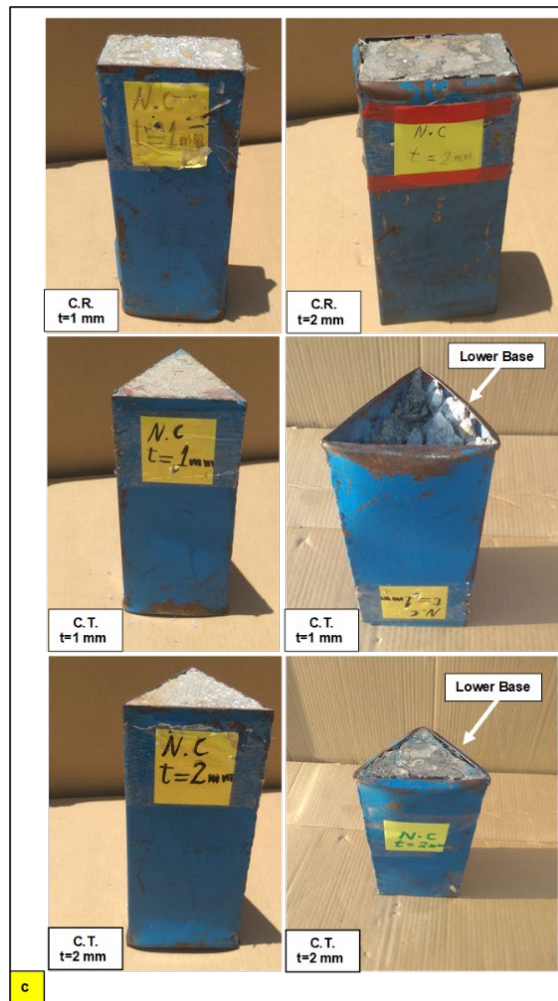


**Figure 16c. Failure patterns of tested RACFST columns of a rectangle and triangle cross-section of steel tube thickness  $t = 1$  and  $2$  mm.**

### 3.3. Load-Deformation Relationship Curves

Fig. 17 shows the plots of experimental axial load ( $N$ ) versus axial deformation ( $DI$ ) in the axial (load – displacement) curve for each of the RACFST columns tested, which included both; an elastic phase and an elastic-plastic phase until to get the failure load. These diagrams show the stages of development of the axial load applied to the samples until the external local buckling of the RACFST is obtained up to the final strength of the column and beyond.

The maximum axial load capacity of the cross-section related by the tested RACFST circular column and its slope in the relation of axial (load – displacement) curves was higher than all other RACFST columns as shown in Fig. 17. Anyway, the ultimate failure load here is not possible to be applied as a method of evaluation between the samples. This fact is because all the tested columns differ from each other in the concrete cross-section area of each column due to maintaining an equal cross-section area for all hollow steel tubes during the design despite the different shapes of these sections. Therefore, ultimate stresses in serviceability limits. This means using 80 % of the value of  $N_u$  to compute the values of these stresses-were used to compare all RACFST columns, which are discussed later in detail.

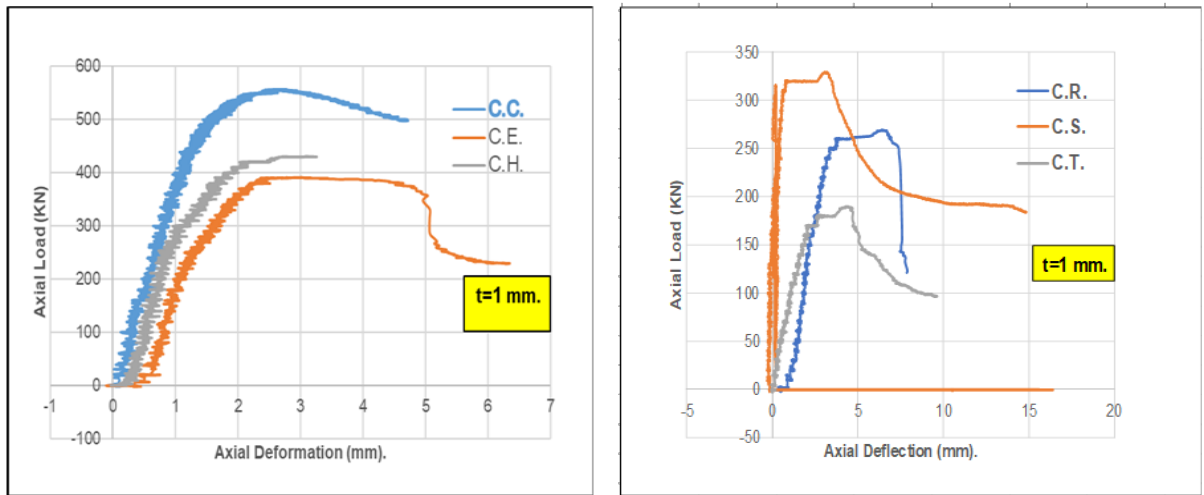


Figure 17a. Diagrams of axial load ( $N$ ) versus axial deformation ( $DI$ ) of RACFST columns with steel tube thickness  $t = 1$  mm.

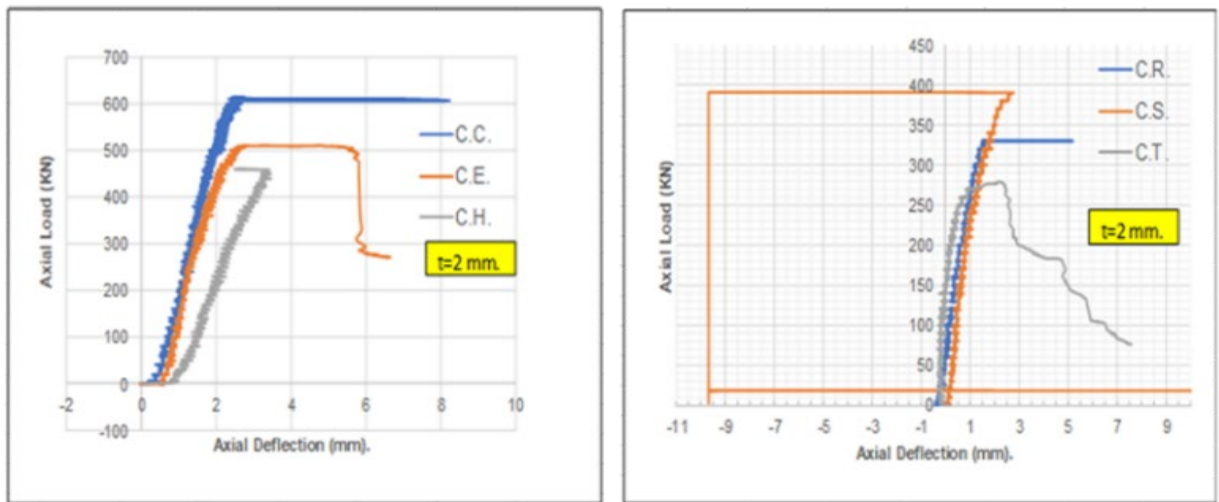


Figure 17b. Diagrams of axial load ( $N$ ) versus axial deformation ( $DI$ ) of RACFST columns with steel tube thickness  $t = 2$  mm.

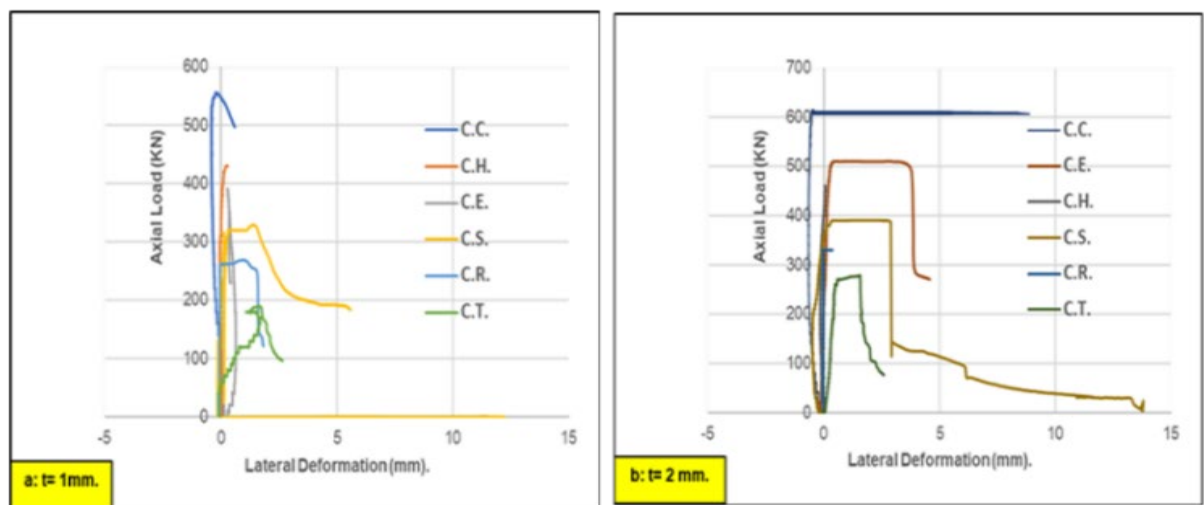
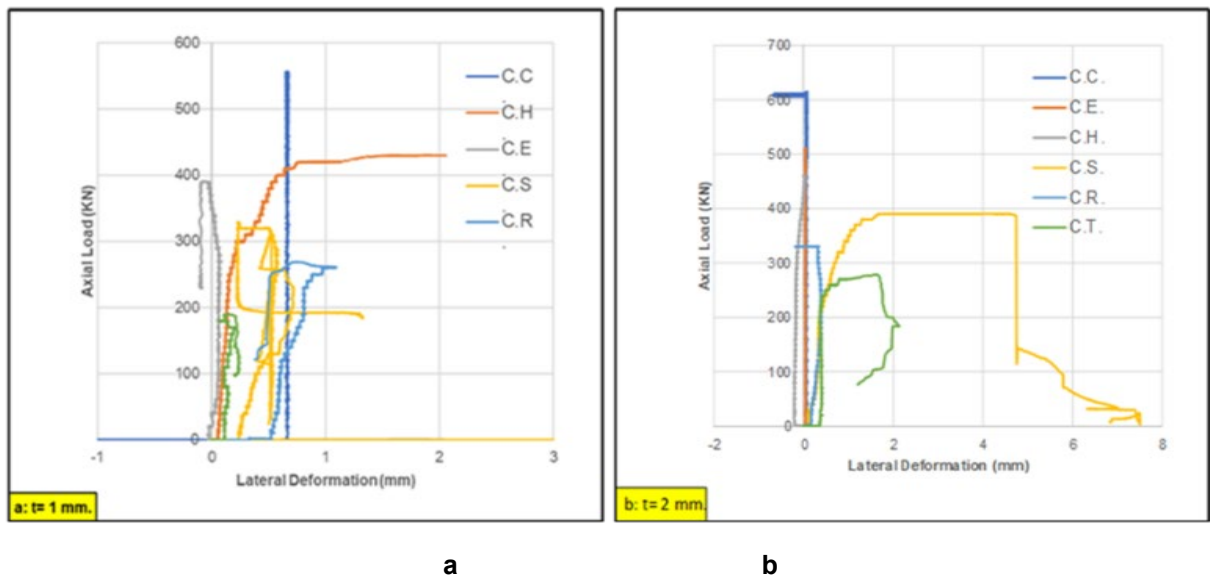


Figure 18. Diagrams of axial load ( $N$ ) versus lateral deformation ( $D2$ ) of all RACFST columns: a –  $t = 1$  mm; b –  $t = 2$  mm.

As shown in Fig. 14, the LVDT positions were installed at the mid-height of the tested RACFST columns. Thus, the relationship was drawn linking the  $N_u$  with the lateral deformation ( $D_2$ ) that occurred in the mid-height of the specimens as illustrated in Fig. 18.

The lateral deflection values were mostly small in the areas close to the middle of the examined RACFST columns. The reason behind this was, initially the application of the load was axial without eccentricity, next, the fact that the columns were short.

During the test and after the applied load reached its maximum value, the outer local buckling developed almost equally around the columns of a symmetrical cross-sectional shape. Then, the lateral displacement developed significantly after reaching the post-peak stage. Moreover, it was observed that the RACFST column with a hexagonal cross-section had lower lateral deformation values compared to other columns for both G1 and G2 groups. Besides, this column showed less damage, after being subjected to concentrated axial loading up to the failure stage of the columns. In addition, The RACFST column with a triangular cross-sectional shape had the highest values of transverse deformation, which were related to the failure patterns of these columns. In general, increasing the steel tube thickness in these columns resulted in a decrease in transverse deformation values.



**Figure 19. Diagrams of axial load ( $N$ ) versus lateral deformation ( $D_3$ ) of all RACFST columns: a –  $t = 1$  mm; b –  $t = 2$  mm.**

Fig. 19 shows the relationship between  $N_u$  with lateral deformation ( $D_3$ ) that occurred in the mid-height of the specimens. It was observed that the transverse deformation values of the RACFST columns with circular and elliptical cross-sections were constant, which is due to the positions of the LVDT devices were perpendicular to the longitudinal welding of these models. That is, the longitudinal welding in this case gave additional strength to the steel tubes, which made the transverse deformation values to be constant throughout the period of applying the vertical load. In general, the transverse deformation values of models with 2 mm thick steel tubes were lower than their 1 mm thick counterparts.

Based on the above information, it can be said that the cross-sectional shape of the RACFST columns did not affect obviously, the relationship of the load versus lateral displacement of the column. Except for the behavior of the RACFST column with a hexagonal cross-section shape which showed less damage, and has lower values of transverse deformation than other columns.

### 3.4. *Ultimate Axial Failure Load of RACFST Columns with Thickness of Steel Tube $t = 1$ and $2$ mm*

The results of laboratory tests of RACFST columns of various cross-sectional shapes with tube thicknesses 1 and 2 mm have been recorded in Table 11. These columns were filled with NSC, using RCA, and were subjected to concentric loads. The results showed that the  $N_u$  was for the circular section column and the lowest for the triangular section column. All the maximum axial loads were represented graphically as shown below in Fig. 20.

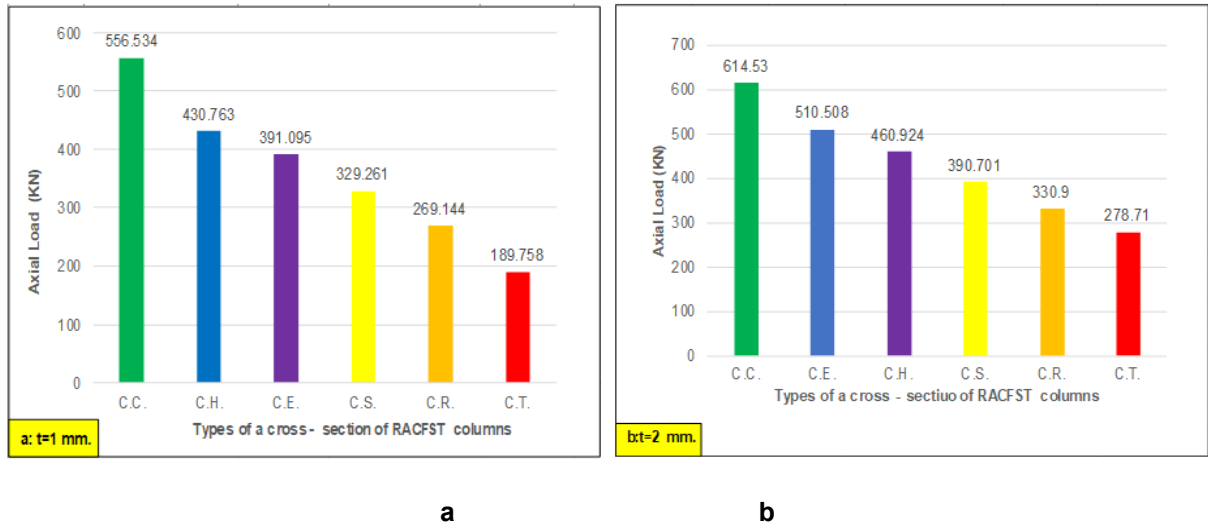


Figure 20. Ultimate axial failure load of all RACFST columns: a –  $t = 1$  mm; b –  $t = 2$  mm.

### 3.5. Effect of Section Shape on Ultimate Stress in Serviceability Limits

As said previously, sections of all RACFST columns were designed with approximately an equal  $P$ , as a result, the cross-section area of the steel tube was approximately equal for all columns. On the other hand, this led to a difference in the cross-section area of the concrete. Thus, it is suitable to calculate the strength for all RACFST columns by using the ultimate stress in serviceability limits. This means using 80 % of the value of  $N_u$  – to compute the values of these stresses, which happened in each column to compare all RACFST columns. These stresses were computed by converting the composite section into an equivalent section of steel to evaluate these columns rather than depending on the ultimate failure axial load. The ultimate stress  $\delta u$  in serviceability limits is calculated by the following Equation [8, 34]:

$$\delta u = \frac{N}{At}, \tag{1}$$

where:  $At = A_s + A_c/n$ ,  $n = E_s/E_c$ ,  $N$  equal to the 80 % of the ultimate failure axial load per column of RACFST columns obtained through the experiment,  $At$  represents the area of steel which equivalent to the cross-section area of each composite column, while  $n$  represents the modular ratio,  $n = E_s/E_c$ , which equals 9.234 and depend on the properties of the materials used in this investigation. With normal-strength concrete, the elastic modulus has been compared with the ACI-318 [35] formula:

$$E_c = 4700\sqrt{f'_c}. \tag{2}$$

The ultimate stress in serviceability limits  $\delta u$  for each RACFST column is illustrated in Fig. 21.

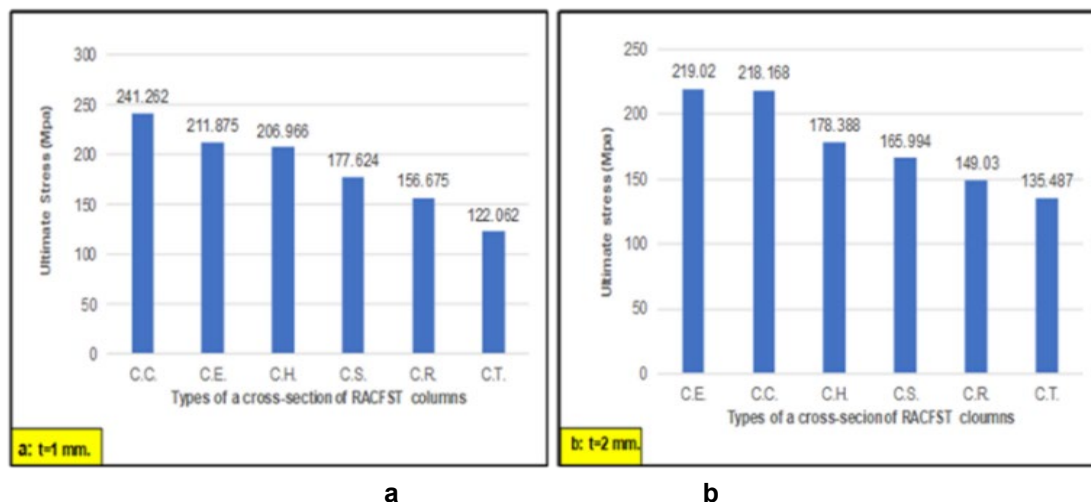


Figure 21. Ultimate stress in serviceability limits of all RACFST columns: a –  $t = 1$  mm; b –  $t = 2$  mm.

In the first group with a thickness of 1 mm, the circular RACFST column showed better confinement of concrete and better bond stress between steel and concrete. It increased the effective compound effect in the member and thus its ability to bear greater ultimate stress in serviceability limits from the other cross-sections shapes of columns such as elliptical, hexagonal, square, rectangle, and triangle. Inversely, the column with a triangle cross-section showed less ability to bear the stress compared with all columns with other sections.

Regarding the second group with a thickness of 2 mm, the results showed that all the columns maintained their arrangement about their ability to withstand ultimate stress in serviceability limits, while the column with an elliptical cross-section showed the ability to bear higher stress than other columns as shown above in Fig. 21.

The RACFST circular column exhibited superior concrete confinement and bond stress between the steel and concrete, leading to increased ability to withstand maximum pressure. The reason for this result was that this column was made of two pieces of steel plates, the dimensions of each piece are 204 × 300 mm, and the dimension of 204 mm has been rotated in a half-circle shape, and 300 mm in height to form half of its circular column. The same work for the second piece so that the circular column is manufactured after welding them symmetrically from both sides along the length of the column. The welding positions of all hollow steel tubes used in this study are illustrated in Fig. 10-8. This rolling process was like a pre-stress for the steel and thus gave the circular shape a greater ability to bear the stress. Besides that, the circular shape was having the ability to generate better confinement of the concrete section compared to other columns sections. The same understanding above applies to the column with an ellipse cross-section.

Regarding the RACFST columns with polygonal sections, Fig. 21 shows that the ultimate stress for RACFST column with hexagonal cross-sectional shape (C.H.) has the highest bearing ultimate stress followed by a square (C.S.), rectangle (C.R.), and then a triangle (C.T.). Thus, a distinctive pattern was observed here with an increasing number of corners of steel plates for the model, that is mean, the greater the number of formed sides and the greater the angles between the sides are 90° or more, have been obtained cross-sectional shape for RACFST column had more stable and confinement, respectively.

For example, the RACFST column with a hexagonal cross-sectional shape showed the highest ultimate stress. This section was made with a circumference of 402 mm equally distributed on six sides with two same sections so that they were symmetrically welded on both sides along the shape. This ribbing process was like a pre-stress work for the steel forming the model, which gave it an additional ability to bear greater stress. Also, the angles between both sides were 120°, which gave the shape greater ability to bear compression. Where the design of this model allowed the concrete components to overlap well with the steel mold, and it also reduced the possibility of occurred decay or gaps between the concrete components and the steel mold during pouring columns. The size of the RCA used in the concrete mix was with a gradient 5–19 mm to comply with the hollow steel tube samples which were made with a small-scale size. Therefore, the measurement of these angles for the RACFST column with a hexagonal cross-sectional shape gave this column a greater ability to withstand the applied compression. By increasing the area of confining the steel cross-section for filled concrete.

As for the square-section column, it had a circumference of 400 mm distributed on four sides, and the width of each side was 100 mm, where the model was made of two halves in the form of L shape. They were welded longitudinally and symmetrically. The same interpretation applies to all RACFST columns with polygonal sections.

### 3.6. Strength Index

The ratio resulting from dividing the value of the ultimate stress of any examined column by the ultimate stress of the circular column is called the strength index (SI) and is used to investigate compression applied. It can be computed from Equation 2 as follows [8, 36]:

$$SI = \frac{\sigma u}{\sigma r}, \quad (3)$$

where  $\sigma u$  represented the ultimate stress for a given column of RACFST columns, whereas  $\sigma r$  represented the ultimate stress of the circular RACFST column. The SI of all tested RACFST columns is shown in Fig. 22, and listed in Table 11. For both groups, the results showed that when the SI values increase, the ultimate stress values for all RACFST columns also increase.

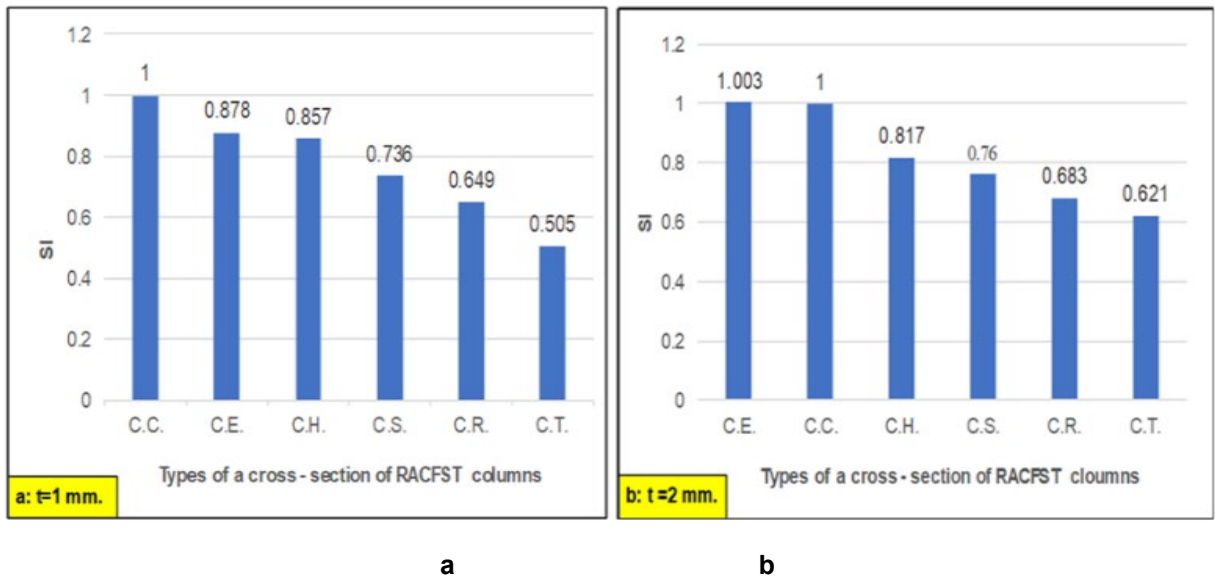


**Figure 22. Strength index of RACFST of all RACFST columns: a – t = 1 mm; b – t = 2 mm.**

### 3.7. Ductility Index

Ductility is a mechanical property of the material that indicates the degree of plastic deformation, as it is considered an effective property of the material. The DI was defined as the ratio of the total axial shortening of a RACFST column as a result of the ultimate failure load during plastic phase loading to axial shortening up to 80 % of the failure load per column. This indicator was defined as reported in [7, 8, 36, 37].

$$DI = \frac{\Delta u}{\Delta 80\%}. \quad (4)$$

The DI values for all tested columns were listed in Table 11 while Fig. 23 showed a graph for these values.

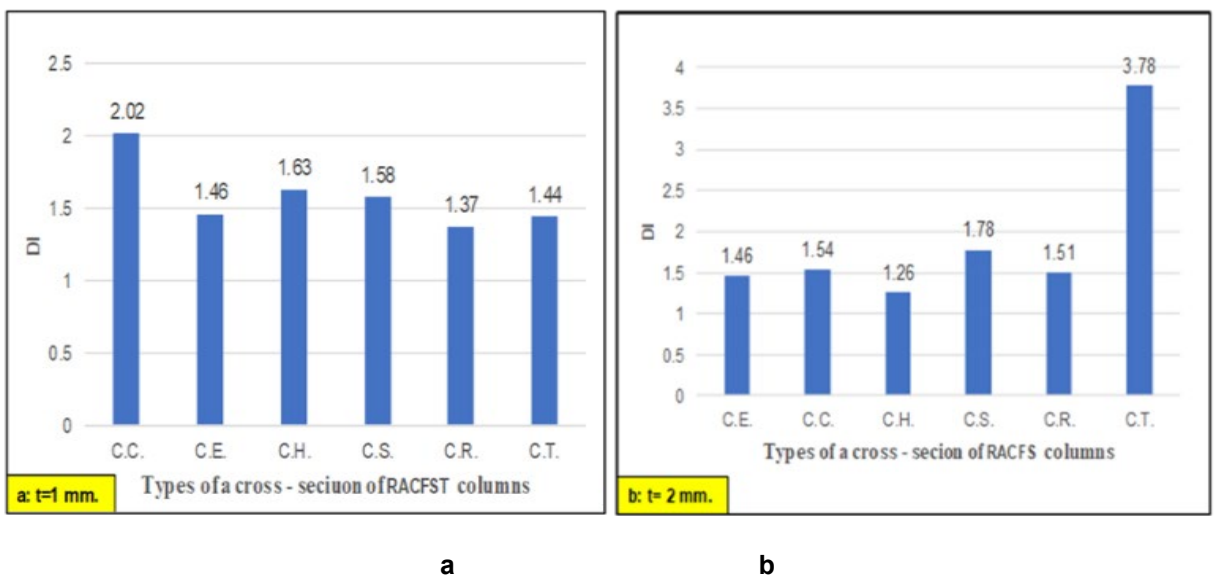


**Figure 23. Ductility index of all RACFST Columns: a – t = 1 mm; b – t = 2 mm.**

Regarding the first group with a thickness of 1 mm, Fig. 23 shows that the DI of the circular column is greater than the ductility of all other shapes, and this is likely due to the good confinement provided by the steel tube with the circular cross-section. This in turn reflects on the failure mechanism of the circular column, which thus determines the value of the DI.

But the RACFST column with a rectangular cross-sectional shape exhibited the smallest value of DI. This is related to the failure pattern of the model, which results from the low capacity to withstand the stress of failure.

As for the second group with a thickness of 2 mm, the DI values for all columns were close except for the triangle column showed a much higher value than the other columns. This result was due to increasing the thickness of the steel 1–2 mm, which led to a decrease in the percentage of concrete contribution ratio (CCR) to bearing the ultimate failure load. Thus, increasing the amount of axial deformation that appeared clearly around the lower perimeter of the base of the triangle column.

While the RACFST column with a hexagonal cross-sectional shape exhibited the smallest value of DI. As a result of the symmetry of its internal ribs and angles, and the fact that the cross-sectional area of the concrete came second after the circular section. These properties for this column increased its ability to withstand ultimate failure stress and thus was reflected in its failure pattern, which did not show obvious deformation during the stages of applying the load.

In addition to that, all RACFST columns, which have conventional cross-sectional shapes such as square and rectangular with a thickness of 2 mm, appear to have high DI than their counterparts with a thickness of 1 mm due to the low CCR. Finally, the elliptical cross-section of RACFST exhibited the stability of the DI value for the two groups, which indicated the stability of the failure pattern of the model in both cases.

### 3.8. Effect of the Thickness of the Steel Tube on

#### 3.8.1. Ultimate axial failure load

For each column, the value of the experimental failure load was obtained. The final values were summarized in Table 11. Also, a comparison was drawn for these  $N_u$  for RACFST by using RCA and for the two groups with thicknesses 1 and 2 mm, and they were illustrated in Fig. 24. As expected, the column strength capacity increased by increasing the thickness of the steel tube for all columns.

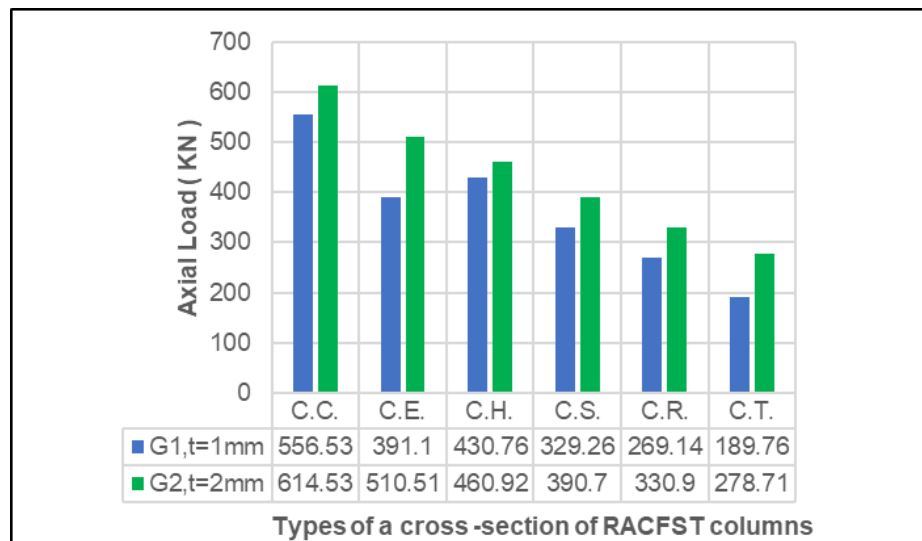
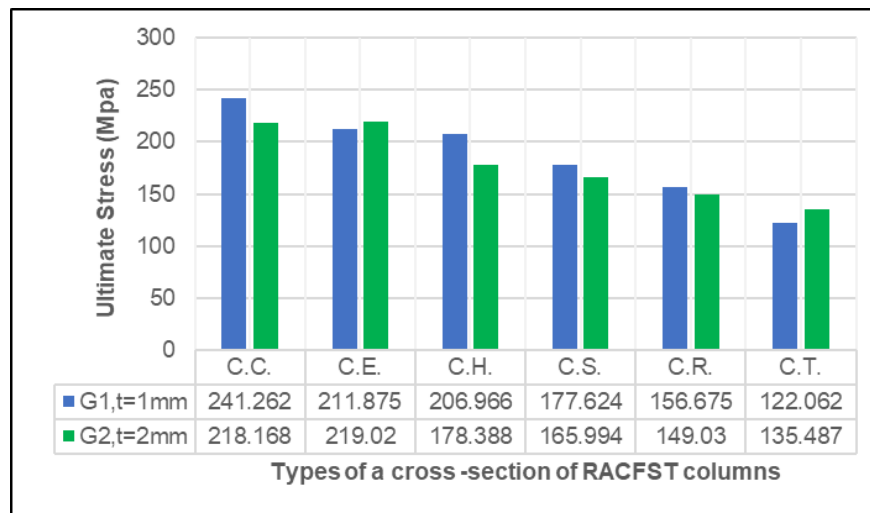


Figure 24. Comparison of the ultimate axial failure load of all RACFST columns.

#### 3.8.2. Ultimate axial stress

The experimental ultimate stress in serviceability limits ( $\delta u$ ) values were obtained for all columns and are listed in Table 11. These values were also compared for the two groups with thicknesses  $t = 1$  and 2 mm and they were drawn in Fig. 25.



**Figure 25. Comparison of the ultimate stress in serviceability limits of all RACFST columns.**

### 3.8.3. Concrete contribution ratio

The contribution of filled concrete for all specimens was analyzed using the CCR, which can be calculated from Equation (4) as reported in [7, 37]:

$$C.C.R. = \frac{N_{exp.}}{A_{s, eff} \cdot f_y}, \quad (5)$$

where  $N_{exp.}$  represented the experimental ultimate failure load;  $A_{s, eff}$ , expresses the effective cross-sectional area of the steel tube as stated by the Eurocode 3 model as reported in [38, 39], and  $f_y$  represented the yield strength of the steel tube. The values of CCR were calculated for each column and their values are recorded in a Table 11 for both groups.

The results, which have been obtained, support what was noted for the failure load. As expected, the CCR of RACFST columns with a steel tube thickness of 2 mm decreases as a result of the practical increase in the cross-sectional area of the steel. Regarding RACFST columns with triangular cross-sections, the CCR values were the lowest, due to the smaller concrete area compared to the other columns.

In general, for the two groups with a thickness of 1 and 2 mm, the results showed that the higher values of CCR led to an increase in the values of SI, accompanied by an increase in the values of ultimate stresses for all specimens. But by comparing the columns with the same sections, it was found that when the thickness of the steel tube increased, this led to a decrease in the values of CCR and thus a decrease in the ultimate stress for these columns due to the increase in the cross-section area for the steel tube.

## 4. Conclusion

This manuscript showed an experimental study of the behavior of twelve RACFST short columns under concentric axial loads. Two groups of thin-walled steel tubes with a thickness of 1 and 2 mm for different shapes of cross-sections were studied. Depending on the analysis of the data obtained from the investigational work of this study, the observing conclusions below were obtained.

1. For all the tested RACFST short columns have been behaved, ductile failure was noticed. The tested short RACFST columns failed due to the internal cracking that occurred in the core of the concrete and then the crash of the recycled concrete – where the sounds of this crashed concrete were heard when exceeding the middle stages of loading – and then the lateral expansion. Continuing with the loading, a local outward buckling occurred near the middle of the RACFST columns as a result of the thin steel plates yielding. In the later stages of the applied loading, more external local buckling occurred near the top and bottom edges of the tested columns.
2. The shape of the cross-section of the RACFST column had a clear effect on the failure patterns that occurred in the tested samples, where the failure pattern of the columns with polygonal cross-sections such as hexagonal, and rectangular were slightly different from the failure pattern of the columns with circular or elliptical sections. But the failure pattern was so different in the RACFST column with a square cross-section where multiple local buckling occurred, starting from the end of the upper third of the column to its end. Also, the RACFST column with a triangular sectional shape

had behaviour not similar to the remaining shapes. Where the local buckling occurred along the lower circumference of the base of the column.

3. Regarding the cross-sectional shape of the RACFST columns, no clear effect on the relationship between load and lateral displacement was observed. Except for the behaviour of the RACFST column with a hexagonal cross-section shape, which showed less damage, and has lower values of transverse deformation than other columns. After being subjected to concentric axial loading up to the failure stage of the columns. On the other hand, and in general, it was found that an increase in the thickness of the steel tube for these columns, results in lower values of transverse deformation.
4. Regarding both groups G1 and G2 with steel plate thickness 1 and 2 mm, RACFST circular and elliptical columns, respectively, showed better stability and confinement of concrete, and the ability to withstand greater ultimate stress in serviceability limits. Thus, these shapes can create better confinement of the concrete section compared to other column sections.
5. The results exhibited that the order of all tested RACFST columns with polygonal cross sections concerning the ultimate stress in serviceability limits was as follows: hexagonal (C.H.), square (C.S.), rectangle (C.R.), and triangle (C.T.). The order of capacity for these columns firstly was due to the increase in the number of ribs of steel plates that were being formed to form the model, secondly, the greater the angle between the sides of the steel plates, which formed the model  $90^\circ$  or more, the model can achieve additional stability and confinement.
6. When the angles between the sides of steel plates, which formed the model, were  $120^\circ$  or more as in the RACFST column with a hexagonal cross-sectional shape, these angles gave the column additional ability to resist the axial load, by allowing the concrete components to overlap well with the steel mold, during pouring specimens to be examined. Thus, the possibility occurred decay or gaps between the concrete components and the steel tube is less.
7. It was found that the ultimate stress values of these RACFST composite columns decrease with the increase in the thickness of the steel tube 1–2 mm due to the increase in the steel section area.
8. When the thickness of the steel tube increases, the CCR value decreases due to the practical increase in the cross-sectional area of the steel tube. Finally, this led to a decrease in the ultimate stress for examined specimens.
9. Regarding ductility, all RACFST columns for both groups with a circular section exhibited high-level ductile behaviour amongst wholly other shapes, whereas columns with a rectangle (C.R.) shaped cross-section exhibited a low-level rate of ductility. In addition to that, columns with conventional cross-section shapes that are circular and squared look to have a comparatively high value of DI.

## References

1. Devi, S.V., Singh, T.G., Singh, K.D. Cold-formed steel square hollow members with circular perforations subjected to torsion. *Journal of Constructional Steel Research*. 2019. 162. Article no. 105730. DOI: 10.1016/j.jcsr.2019.105730
2. Han, L.H., Li, W., Bjorhovde, R. Developments and advanced applications of concrete-filled steel tubular (CFST) structures: Members. *Journal of Constructional Steel Research*. 2014. 100. Pp. 211–228. DOI: 10.1016/j.jcsr.2014.04.016
3. Gabel, J., Carver, M., Gerometta, M. The Skyscraper Surge Continues, The 'Year of 100 Supertalls.' *CTBUH Journal*. 1(2016). 38–45.
4. Han, L.H., An, Y.F. Performance of concrete-encased CFST stub columns under axial compression. *Journal of Constructional Steel Research*. 2014. 93. Pp. 62–76. DOI: 10.1016/j.jcsr.2013.10.019
5. Ren, Q.X., Han, L.H., Lam, D., Li, W. Tests on elliptical concrete filled steel tubular (CFST) beams and columns. *Journal of Constructional Steel Research*. 2014. 99. Pp. 149–160. DOI: 10.1016/j.jcsr.2014.03.010
6. Hassanein, M.F., Patel, V.I., Bock, M. Behaviour and design of hexagonal concrete-filled steel tubular short columns under axial compression. *Engineering Structures*. 2017. 153. Pp. 732–748. DOI: 10.1016/j.engstruct.2017.10.010
7. Ibañez, C., Hernández-figueirido, D., Piquer, A. Shape effect on axially loaded high strength CFST stub columns. *Journal of Constructional Steel Research*. 2018. 147. Pp. 247–256. DOI: 10.1016/j.jcsr.2018.04.005
8. Almamoori, A.H.N., Naser, F.H., Dhahir, M.K. Effect of section shape on the behaviour of thin walled steel columns filled with light weight aggregate concrete: Experimental investigation. *Case Studies in Construction Materials*. 2020. 13. Article no. e00356. DOI: 10.1016/j.cscm.2020.e00356
9. Bahrami, A., Kouhi, A.M. Compressive Behaviour of Circular, Square, and Rectangular Concrete-Filled Steel Tube Stub Columns. *Civil Engineering and Architecture*. 2020. 8(5). 1119–1126. DOI: 10.13189/cea.2020.080538
10. Ceia, F., Raposo, J., Guerra, M., Júlio, E., De Brito, J. Shear strength of recycled aggregate concrete to natural aggregate concrete interfaces. *Construction and Building Materials*. 2016. 109. Pp. 139–145. DOI: 10.1016/j.conbuildmat.2016.02.002
11. Kou, S.C., Poon, C.S. Enhancing the durability properties of concrete prepared with coarse recycled aggregate. *Construction and Building Materials*. 2012. 35. Pp. 69–76. DOI: 10.1016/j.conbuildmat.2012.02.032
12. Li, X. Recycling and reuse of waste concrete in China. Part I. Material behaviour of recycled aggregate concrete. *Resources, Conservation and Recycling*. 2008. 53(1–2). Pp. 36–44. DOI: 10.1016/j.resconrec.2008.09.006
13. Lye, C.Q., Dhir, R.K., Ghataora, G.S., Li, H. Creep strain of recycled aggregate concrete. *Construction and Building Materials*. 2016. 102(1). Pp. 244–259. DOI: 10.1016/j.conbuildmat.2015.10.181

14. Ma, H., Xue, J., Zhang, X., Luo, D. Seismic performance of steel-reinforced recycled concrete columns under low cyclic loads. *Construction and Building Materials*. 2013. 48. Pp. 229–237. DOI: 10.1016/j.conbuildmat.2013.06.019
15. Silva, R.V., De Brito, J., Dhir, R.K. Establishing a relationship between modulus of elasticity and compressive strength of recycled aggregate concrete. *Journal of Cleaner Production*. 2016. 112(4). Pp. 2171–2186. DOI: 10.1016/j.jclepro.2015.10.064
16. Thomas, C., Setián, J., Polanco, J.A., Alaejos, P., Sánchez De Juan, M. Durability of recycled aggregate concrete. *Construction and Building Materials*. 2013. 40. Pp. 1054–1065. DOI: 10.1016/j.conbuildmat.2012.11.106
17. Chen, Z., Xu, J., Chen, Y., Lui, E.M. Recycling and reuse of construction and demolition waste in concrete-filled steel tubes: A review. *Construction and Building Materials*. 2016. 126. Pp. 641–660. DOI: 10.1016/j.conbuildmat.2016.09.063
18. Chen, Z., Xu, J., Xue, J., Su, Y. Performance and calculations of recycled aggregate concrete-filled steel tubular (RACFST) short columns under axial compression. *International Journal of Steel Structures*. 2014. 14(1). Pp. 31–42. DOI: 10.1007/s13296-014-1005-5
19. Safiuddin, M., Alengaram, U.J., Rahman, M.M., Salam, M.A., Jumaat, M.Z. Use of recycled concrete aggregate in concrete: A review. *Journal of Civil Engineering and Management*. 2013. 19(6). Pp. 796–810. DOI: 10.3846/13923730.2013.799093
20. De Azevedo, V. da S., De Lima L.R.O, Vellasco, P.C.G. da S., Tavares, M.E. da N., Chan, T.-M. Experimental investigation on recycled aggregate concrete filled steel tubular stub columns under axial compression. *Journal of Constructional Steel Research*. 2021. 187. Article no. 106930. DOI: 10.1016/j.jcsr.2021.106930
21. Yang, Y.-F., Han, L.-H. Experimental behaviour of recycled aggregate concrete filled steel tubular columns. *Journal of Constructional Steel Research*. 2006. 62(12). 1310–1324. DOI: 10.1016/j.jcsr.2006.02.010
22. Yang, Y.-F., Han, L.-H. Compressive and flexural behaviour of recycled aggregate concrete filled steel tubes (RACFST) under short-term loadings. *Steel and Composite Structures*. 2006. 6(3). 257–84. DOI: 10.12989/scs.2006.6.3.257
23. Chen, Z.-P., Chen, X.-H., Ke, X.-J., Xue, J.-Y. Experimental study on the mechanical behavior of recycled aggregate coarse concrete-filled square steel tube column. 2010 International Conference on Mechanic Automation and Control Engineering. Wuhan, 2010. Pp. 1313–1316. DOI: 10.1109/MACE.2010.5536341
24. Li, W., Xiao, J., Shi, C., Poon, C.S. Structural Behaviour of Composite Members with Recycled Aggregate Concrete – An Overview. *Advances in Structural Engineering*. 2015. 18(6). 919–938. DOI: 10.1260/1369-4332.18.6.919
25. Wang, Y., Chen, J., Geng, Y. Testing and analysis of axially loaded normal-strength recycled aggregate concrete filled steel tubular stub columns. *Engineering Structures*. 2015. 86. 192–212. DOI: 10.1016/j.engstruct.2015.01.007
26. Niu, H.-C., Cao, W.-L. Full-scale testing of high-strength RACFST columns subjected to axial compression. *Magazine of Concrete Research*. 2015. 67(5). 257–270. DOI: 10.1680/macr.14.00198
27. Lyu, W.-Q., Han, L.-H., Hou, C. Axial compressive behaviour and design calculations on recycled aggregate concrete-filled steel tubular (RAC-FST) stub columns. *Engineering Structures*. 2021. 241. Article no. 112452. DOI: 10.1016/j.engstruct.2021.112452
28. Yang, D., Liu, F., Wang, Y. Axial compression behaviour of rectangular recycled aggregate concrete-filled steel tubular stub columns. *Journal of Constructional Steel Research*. 2023. 201. Article no. 107687. DOI: 10.1016/j.jcsr.2022.107687
29. Mohammed, K., Alnebbhan, J. Behaviour of concrete filled steel tube truss girder with deck slab. College of Engineering of the University of Al-Qadisiyah, 2020.
30. Abbas, A.W. Reactive Powder Concrete- Filled Double Skin Tubular Column Subjected to Repeated Loading. Kerbala University/College of Engineering, 2021. 201 p.
31. ASTM A370-22. Standard test methods and definitions for mechanical testing of steel products. ASTM Int. 2022;01.03(Reapproved):1–48.
32. Sureshkumar, M.P., Sathish Kumar, B., Ravikanth, J. Green Concrete – A Review. *International Research Journal of Multidisciplinary Technovation*. 2019. 1(6). Pp. 458–464. DOI: 10.34256/irjmtcon64
33. Majid, A., Aoun, A. Comparative Study for Different Types of Reinforced Concrete Spliced Girders. Kerbala University/College of Engineering, 2018. 182 p.
34. Ren, Q.-X., Han, L.-H., Lam, D., Hou, C. Experiments on special-shaped CFST stub columns under axial compression. *Journal of Constructional Steel Research*. 2014. 98. 123–133. DOI: 10.1016/j.jcsr.2014.03.002
35. Wight, J.K., Barth, F.G., Becker, R.J., Bondy, K.B., Breen, J.E., Cagley, J.R., et al. Building Code Requirements for Structural Concrete (ACI 318-05) and Commentary (ACI 318R-05). ACI Committee 318, 2004, 2003.
36. Jain, S., Chellapandian, M., Prakash, S.S. Emergency repair of severely damaged reinforced concrete column elements under axial compression: An experimental study. *Construction and Building Materials*. 2017. 155. 751–761. DOI: 10.1016/j.conbuildmat.2017.08.127
37. Pansuriya, D., Panchal, V.R., Panchal, D.R. Experimental Study on Comparison of Square, Rectangular and Circular Concrete Filled Steel Tube Composite Columns. *Journal of Emerging Technologies and Innovative Research*. 2018. 5(7). 988–993.
38. DD ENV1993-1-1:1992. Eurocode 3: Design of steel structures – Part 1.1: General rules and rules for buildings. BSI. London, 2000.
39. Bouaricha, A., Handel, N., Boutouta, A., Djouimaa, S. Load bearing capacity of thin-walled rectangular and i-shaped steel sections of short both empty and concrete-filled columns. *Fattura ed Integrità Strutturale*. 2021. 15(58). 77–85. DOI: 10.3221/IGF-ESIS.58.06

#### **Information about the authors:**

**Abdullah Samir Haitham,**

E-mail: [haitham.a@s.uokerbala.edu.iq](mailto:haitham.a@s.uokerbala.edu.iq)

**Hameed Naser Almamoori Ali,**

E-mail: [haitham.a@s.uokerbala.edu.iq](mailto:haitham.a@s.uokerbala.edu.iq)

Received 15.02.2023. Approved after reviewing 07.10.2024. Accepted 11.06.2025.